Astron. Astrophys. 285, 185–198 (1994)

ASTRONOMY AND ASTROPHYSICS

Stationary boundary layers of accretion α disks: profiles and emission properties

A. Lioure and O. Le Contel

Commissariat à l'Energie Atomique, Centre d'Etudes de Bruyères-le-Châtel, B.P.12, F-91680 Bruyères-le-Châtel, France

Received 4 October 1993 / Accepted 9 November 1993

Abstract. We model stationary profiles of physical quantities in a disk and its boundary layer around an accreting object using the relaxation method. We take into account the full energy equation with dissipation due to differential rotation and energy losses by radiation in the optically thick limit. We use the alpha prescription for the viscosity with a special treatment near the star according to previous works. We restrict ourselves to the subsonic case. We find that the system presents a twofold boundary layer: the usual dynamical one defined by the locus of the maximum rotation rate, and a thermal one, larger, the size of which is determined by an effective Prandtl number. Second, the presence of a radial flux at the inner boundary affects the energy balance. In particular, when energy is radiated into the star, the boundary layer is far from radiating half of the accretion luminosity. The spectral distribution of the emitted energy of the whole structure shows two components: in addition to the classical disk spectrum, there is a high energy part corresponding to the thermal boundary layer. The high energy excess due to the boundary layer can be either very strong or very weak, depending on the values of the model parameters. The more realistic spectral distribution corresponds to fairly low boundary layer luminosities. We apply this to the case of DF Tau.

Key words: accretion disks – stars: DF Tau – stars: pre-main sequence – circumstellar matter

1. Introduction

Calculating the radial profiles of physical quantities of an accretion disk is difficult, especially in the vicinity of the central object and when a so-called boundary layer is to be expected, due to the slow rotation of the former with respect to the break-up velocity. The pioneering work by Shakura & Sunyaev (1973) suffered from the disease of assuming both keplerian velocity and no-torque condition at the inner boundary. These two contradictory conditions lead, of course, to unrealistic profiles near the center. But their point was not to compute exactly the central region but much more to have a good description of the external parts of the accretion disk. However, in many astrophysical cases it is indispensable to model as precisely as possible the inner parts of the disk, including the boundary layer if one wants to know its emission properties. Many of the enlightening ideas that are used today date back to Lynden-Bell & Pringle (1974). They emphasized key questions as the boundary layer thickness and temperature and realized that the viscosity had to diminish there in order to yield geometrically thin boundary layer, but we still lack exact calculations, even in the one-dimensional approximation, which give these physical quantities in a self-consistent way and draw observational consequences.

Stationary calculations were undertaken some time ago by Regev (1983) using the matched asymptotic expansion method (MAE). This method has the great advantage of being of low computational cost and largely analytical. Moreover, the physics appears much more clearly because of the assumptions one is lead to make. One shortcoming of this method lies in the fact that it is unable to treat very accurately the region where the rotational velocity reaches its maximum, that is precisely the most delicate region of the structure. However, these drawbacks could be overcome by a more refined mapping of the radial axis. The relaxation method seems to be much better adapted to the problem and was actually used recently in the work of Paczyński (1991) and Popham & Narayan (1991) who solved without matching the equations of the disk structure in the polytropic approximation. Although the gas can be shown to behave in a polytropic manner far in the disk, it is no more true near the central object and realistic calculations must include dissipation and radiation. We are aware of a very recent work, made independently by Narayan & Popham (1993), who solved the problem of the disk and boundary layer structure in both optically thin and optically thick cases. Although the aim of our two papers is very similar, some assumptions are different: they consider the disk, the boundary layer and the star as the same fluid, and retain the disk equations to describe the star. As a consequence, the star is considered as a cylindrical object with a constant accretion rate, at least in its outer layers. Because the interaction between a geometrically thin disk with a boundary

Send offprint requests to: A. Lioure

layer and a star is so far unknown, we chose a rather different point of view. In fact we forced the edge of the star to coincide with the inner end of our computational domain and imposed boundary conditions. After the method has converged, we check *a posteriori* that the initial assumptions are not violated: the disk and the boundary layer remain geometrically thin and optically thick.

A number of non-stationary calculations have also been attempted. Papaloizou & Stanley (1986) were the first to use a one dimensional code with a polytropic equation of state. They aimed at finding stationary states of the system if any, and possibly investigating some oscillatory or even unstable configurations. They found that the inner region of the disk as well as the boundary layer were not subject to high amplitude oscillations. Later, Okuda & Mineshige (1991) included energy dissipation and radiation transfer, but without considering the boundary layer. Kley (1991) reports numerical calculations in two dimensions including radiative transfer of an accretion disk and a boundary layer around a cataclysmic variable, trying to solve the problem in a very accurate and complete way. All these numerical calculations are definitely the right track to follow if one wants to know the detailed behaviour of a disk around a star, all the more because it has been shown that instabilities (Blumenthal et al. 1984) may occur that would be very interesting to push in the non-linear regime. However, the difficulty of such calculations makes it very hard to draw any reliable conclusion on the long term evolution or on the possible occurrence of a stationary state of accretion disks and boundary layers.

The importance of magnetic field has been demonstrated (Balbus & Hawley 1991): it can drive powerful instabilities which might transport angular momentum outward and thus start accretion through a non-viscous phenomenon. Besides, magnetic fields are observed around T-Tauri stars. The theory of magnetic accretion disks and boundary layers is to be investigated further.

Although the concept of accretion disk is not universally accepted in the case of T-Tauri stars, it has proved very powerful matching the gross features of emission spectra of many young stars as well as binary systems, and in some cases is actually observed (Sargent & Beckwith 1987, Malbet et al. 1993). A few of these objects desperately need another interpretation of their abnormal spectra (RY Tau and T Tau: Bertout et al. 1988). In the case of binary systems, high spatial resolution observations are possible due to the eclipse phenomenon, and one can now trace physical properties of the material flowing from the secondary star to the primary almost to the surface and fit them reasonably to the predictions of an active accretion disk model (Horne & Cook 1985). One can in principle infer from these observations unknown parameters like the accretion rate. However, the boundary layer properties are usually modelled in a very simple way.

We report in this paper a numerical study of one-dimensional, stationary, non-magnetic accretion disks and boundary layers. These three approximations are crude in a real context where oscillations and MHD instabilities probably occur in the disk and where the boundary layer might be geometrically thick. Moreover, the star is supposed to be static and at constant temperature in its outer layers. However, in these calculations, the boundary layer is calculated in a self-consistent way and some interesting results arise that might not be affected qualitatively in more realistic simulations. In particular, the outgoing spectrum of a self-consistently calculated boundary layer is shown and we find that one has to be careful in deriving the boundary layer luminosity because it can be significantly different from the usual estimate of the standard model. In Sect. 2, we present our model and method of solution. We describe the results obtained and observational implications in Sects. 3 and 4. Finally, Sect. 5 is devoted to discussion and prospects.

2. The model

2.1. The equations

Since the equations of axisymmetric accretion flows have been extensively described in the literature, we are not going to give any details on the way to derive them (See for example Lynden-Bell & Pringle (1974)). We integrated the equations over the vertical variable z to get the surface density $\Sigma = \int_{-\infty}^{+\infty} \varrho(R,z)dz$, and assumed that the radial and azimutal velocities depend only on the radial coordinate; we also considered the temperature as being the central temperature. The way to include the vertical structure is as usual to assume hydrostatic equilibrium which gives the local scale height, H, in terms of local sound speed and keplerian rotation rate:

$$H = \frac{C_s}{\Omega_K}.$$

We supposed that this is still true in the boundary layer, and checked the validity of the approximation *a posteriori*. We made the assumption of optical thickness for all the structure from far away the central object down to its surface, giving the following formulae for the radiative fluxes in both directions, in the diffusion approximation:

$$F_z = -\frac{16\sigma}{3}\frac{T^3}{\kappa_r \varrho}\frac{\partial T}{\partial z},$$

$$F_R = -\frac{16\sigma}{3}\frac{T^3}{\kappa_r \varrho}\frac{\partial T}{\partial R}.$$

The z-averaging of the radial flux,

$$\int_{-\infty}^{+\infty} \frac{1}{R}\partial_R(RF_R)dz,$$

is approximated by :

$$\frac{1}{R}\partial_R(2HRF_R),$$

and the vertical flux is taken to be:

$$F_z = \frac{16\sigma}{3}\frac{T^4}{\kappa_r \varrho H},$$

over the midplane. In each case, κ_r is the Rosseland mean for the opacity. We used the Kramers law for the opacity: $\kappa_r = 0.11 n T^{-3.5} \mathrm{cm}^2 \mathrm{g}^{-1}$. This law is valid for the case of white dwarfs, but probably not for the much lower temperatures involved in the disk and the boundary layer surrounding a T-Tauri star. However, we intend first to give some insight in the physics of the boundary layer problem and a single opacity law makes it easier to compare the various influences of different parameters. We used a different opacity law to simulate DF-Tauri.

The standard equations then write:

$$\dot{M} = -2\pi R \Sigma u_R \quad (1)$$

$$\Sigma(u_R \partial_R u_R - R\Omega^2) = -\partial_R P - \Sigma \frac{GM_\star}{R^2} \quad (2)$$

$$\Sigma \frac{u_R}{R^2} \partial_R (R^2 \Omega) = \frac{1}{R^3} (\partial_R (\nu \Sigma R^3 \partial_R \Omega)) \quad (3)$$

$$\Sigma C_v (u_R \partial_R T) = -P \left(\frac{1}{R} \partial_R (R u_R) \right) + \nu \Sigma R^2 (\partial_R \Omega)^2 - \frac{2}{R} \partial_R (RHF_R) - 2F_z \quad (4)$$

where each symbol has its usual meaning in accretion disk theory. Note that P is the z-integrated pressure and $\dot{M}$ is taken to be positive. The second equation can be integrated, with an integration constant C, representing the flux of specific angular momentum at the point where $\partial_R \Omega = 0$:

$$\frac{\dot{M}}{2\pi} (\mathrm{C} - R^2 \Omega) = \nu \Sigma R^3 \partial_R \Omega$$

2.2. Scaling of the physical quantities

We used a non-dimensional form of these equations with scaling quantities chosen to be as close as possible to the standard model.

$$R_{dim} = R_\star$$

$$\Omega_{dim} = \Omega_{K\star} = \sqrt{\frac{GM_\star}{R^3}}$$

$$\frac{32 T_{dim}^4}{3\tau_{dim}} = \frac{3GM\dot{M}}{8\pi\sigma {R_\star}^3} \quad (5)$$

$$u_{dim} = \left(\frac{1}{(\gamma-1)} \frac{k_B T_{\mathrm{dim}}}{\mu} \right)^{1/2} = \left(\frac{1}{(\gamma-1)} \right)^{1/2} C_{s\ dim}$$

$$H_{dim} = \frac{u_{dim}}{\Omega_{dim}}$$

$$\Sigma_{dim} = \frac{\dot{M}}{2\pi H_{dim} u_{dim}} \quad (6)$$

$$\varrho_{dim} = \frac{\Sigma_{dim}}{2H_{dim}}$$

$$\tau_{dim} = \kappa_{dim} \Sigma_{dim}$$

where k_B is the Boltzmann constant and μ is the mean molecular weight of the gas, and $C_{s\ dim}$ the dimensional isothermal sound speed.

These relations are in fact a system to be solved because the temperature and surface density are given in an implicit way by Eqs. 5 and 6, exactly like in Shakura & Sunyaev (1973). This gives the following explicit form for the temperature in the case where the opacity reads $\kappa = \kappa_0 \varrho^n T^q = \kappa_0 \left(\frac{\Sigma}{2H}\right)^n T^q$, and if $u_{dim} = c_0 \sqrt{T_{dim}}$:

$$T_{dim} = \left(\frac{9\kappa_0 \dot{M}^{n+2} {\Omega_{dim}}^{2n+3}}{2^{2n+9} \pi^{n+2} c_0^{3n+2} \sigma} \right)^{\frac{2}{3n+10-2q}}$$

In our case, n=1 and q = -3.5, thus

$$T_{dim} \sim \dot{M}^{3/10} M_\star^{1/4} R_\star^{-3/4}$$

With this choice, the z-integrated non-dimensional pressure is measured in units of $\Sigma_{dim} u_{dim}^2$, the internal specific energy in units of u_{dim}^2, and the viscosity ν in units of $c_{dim} H_{dim}$. In particular, the equation of state expressed in these non-dimensional variables, noted in small letters, reads:

$$p = (\gamma - 1)\Sigma t$$

The dimensional parameters are related to the physical problem we examine: T-Tauri star or white dwarf. The typical figures we took to run calculations are listed in Table 1.

Two non-dimensional numbers appear in the equations:

$$\mathscr{M}_{dim} = \frac{R_{dim}}{H_{dim}} = \frac{R_{dim} \Omega_{dim}}{u_{dim}},$$

and

$$\mathscr{P}_{dim} = \frac{3}{16\sigma} \frac{\kappa_{dim} \varrho_{dim} \Sigma_{dim} {u_{dim}}^3}{{T_{dim}}^4} = \frac{4}{3}.$$

The former is the typical azimutal Mach number, high in thin disk theory. Let us explicitly write how it depends on the physical parameters of the flow:

$$\mathscr{M}_{dim} \sim \dot{M}^{-3/20} M_\star^{3/8} R_\star^{1/8}$$

The latter is linked to the radiative terms and corresponds naturally to a typical Prandtl number $\mathscr{P}_{dim}$ of the flow, expressing the relative importance of viscous transport over radiative transport. Due to our choice of the scaling quantities, it is in fact very close to the real Prandtl number of alpha-disks which happens to be a constant very close to 1 (see Sect. 3). These two numbers can be related to the ones of the Regev study (1983), but with a different interpretation:

$$\mathscr{P}_{dim} = \frac{1}{\eta} \qquad \mathscr{M}_{dim} = \frac{1}{\epsilon}$$

Let us note also that the non-dimensional accretion rate, expressed in units of $2\pi u_{dim} \Sigma_{dim} R_{dim}$ is a constant and reads:

$$\dot{m} = \frac{1}{\mathscr{M}_{dim}}.$$

Table 1. Typical values of parameters for T-Tauri stars and white dwarfs

	R_{dim}	$\dot{M}$	$M_\star$	$T_\star$	$\Omega_\star$	$\mathscr{M}_{dim}$	α	λ_{dim}	L_{acc}
T-Tauri	$4.3R_\odot$	$10^{-7}M_\odot yr^{-1}$	$1M_\odot$	5000K	$0.1\Omega_K$	24.15	10^{-2}	0.5 μm	2.96 $10^{33} ergs\ s^{-1}$
White Dwarf	9000 km	$4.10^{-9}M_\odot yr^{-1}$	$1M_\odot$	10^5K	$0.1\Omega_K$	80.64	10^{-2}	0.14 μm	3.94 $10^{34} ergs\ s^{-1}$

We will also write $\mathscr{C}$ for the non-dimensional integration constant C:

$$\mathscr{C} = \frac{\mathrm{C}}{\mathrm{R}_{\mathrm{dim}}^2 \Omega_{\mathrm{dim}}},$$

the angular momentum flowing through the dynamical boundary layer limit, considered as a parameter.

The previous three equations become, after some work, a system of four first order equations which is the one we integrated (all quantities being non dimensional):

$$\partial_r \omega = -(r^2\omega - \mathscr{C})\frac{1}{\nu\Sigma r^3}, \tag{7}$$

$$\partial_r t = -\frac{\kappa\Sigma}{rh^2t^3}(rhf_r), \tag{8}$$

$$\partial_r(rhf_r) = r\mathscr{M}_{dim}^2[-\frac{t^4}{\kappa\Sigma} + \frac{\mathscr{P}_{dim}}{2}(\nu\ \Sigma\ (r\partial_r\omega)^2 + \frac{1}{r\mathscr{M}_{dim}^2}(\partial_r t - (\gamma-1)t\frac{\partial_r\Sigma}{\Sigma}))], \tag{9}$$

$$\partial_r\Sigma = (\mathscr{M}_{dim}^2\ (\ r\omega^2 - \frac{1}{r^2}) - (\gamma-1)\partial_r t + (\frac{1}{r\Sigma\mathscr{M}_{dim}})^2\frac{1}{r})\Sigma \Big/ \left((\gamma-1)t - (\frac{1}{r\Sigma\mathscr{M}_{dim}})^2\right) \tag{10}$$

Our variables are thus the central temperature, the rotation rate, the surface density and a combination involving the z-integrated radial flux. It is clear from the above system that the solution will depend only on $\mathscr{M}_{dim}$ and boundary conditions for fixed opacity and viscosity prescriptions (see Table 1).

2.3. Viscosity prescription

This is to date one of the most unclear points of accretion disks but we are not going to deal here with the basic physical problem. Since we are in the case of non-magnetic disks, we cannot invoke the Balbus & Hawley (1991) instability mechanism for example. We used the classical turbulent approximation for the viscosity:

$$\nu = \alpha C_s H.$$

However, it has been recognized for a long time (Lynden-Bell & Pringle 1974; Regev 1983; Papaloizou & Stanley 1986) that the viscosity, assumed to be of turbulent origin, had to be different near the star than in the disk, because the typical size of turbulent eddies should not exceed the typical local length scale, smaller in a narrow boundary layer. In fact, an estimate of the radial pressure length scale when the centrifugal force is negligible compared to the gravitational force is $L_P = \frac{H^2}{R}$, thus leading to the following formula for the turbulent viscosity:

$$\nu_{BL} \sim \alpha C_s \frac{H^2}{R}.$$

There is an alternative to this prescription given in Shakura & Sunyaev (1988) where the typical turbulent length scale in the boundary layer is the same as above but a correction is applied to the characteristic turbulent speed. Altogether, this leads to a viscosity prescription of the type:

$$\nu = \alpha C_s H^3/R^2,$$

in the case of a slowly rotating star, which is much smaller (by a factor of order $1/\mathscr{M}_{dim}$). Regev (1983) assumes a constant viscosity in the boundary layer a factor $1/\mathscr{M}_{dim}^2$ lower than its mean value in the disk, always assuming the same typical size for the eddies. This prescription is very close to that proposed by Shakura & Sunyaev (1988) except that the viscosity is then constant. We ran calculations with these three different viscosity prescriptions, the last two ones giving very close results.

2.4. Boundary conditions and free parameters

Since we have four equations, the same number of boundary conditions have to be fixed. We split them into two inner and two outer conditions. At the inner edge, which is meant to represent stellar material, we imposed the rotation rate and the temperature. This temperature is somewhat troublesome physically since the connection between the star and the boundary layer is very unclear: the outer layers of the star are very likely to be perturbed substantially, dynamically as well as thermically. So, choosing a mean stellar atmosphere temperature for the inner boudary condition may be an oversimplification. We varied the boundary temperature in order to display its influence on the boundary layer and give an idea of the potential time dependent evolution of the star. Had we imposed the flux as a boundary condition, this would have raised the same kind of problems. As we expect the behaviour of the solution to be close to the one in Shakura & Sunyaev (1973) far away, we imposed the logarithmic slope of two other quantities at the outer boundary, for example temperature and rotation rate.

In addition there are several free parameters, a few of which can possibly be observed and the others cannot be constrained in any way except by their possible influence on the outgoing spectrum. The constant $\mathscr{C}$ which represents the amount of angular

momentum accreted by the star, the viscosity prescription in the boundary layer , the accretion rate and the α parameter belong to the second kind while the star radius and the star rotation rate may be given by observations.

The consequence of the above discussion is that the system we solve depends on 6 parameters:

- two inner boundary conditions: $T_\star, \Omega_\star$. (The two outer ones are fixed by the standard model)
- $\mathscr{M}_{dim}$
- α and ν_{BL}
- $\mathscr{C}$

Although $\dot{M}, M_\star, R_\star$ only influence the result through the combination involved in $\mathscr{M}_{dim}$, we found it more physical to discuss their role independently in the following.

2.5. Numerical method

This system has proven to be very stiff (see for instance Muchotrzeb & Paczyński 1982) and impossible to be solved with either a standard or implicit Runge-Kutta method. Moreover, several boundary conditions have to be fulfilled and a shooting method should be used combined with the Runge-Kutta. We had, like others (Popham & Narayan 1991; Paczyński 1991), to use the relaxation method which is very powerful in solving stiff problems with boundary conditions. We worked with a fixed grid since we restricted ourselves to subsonic solutions. Had we had to deal with sonic points, it would then have been required to add one further equation for a varying grid (Press et al. 1986).

We chose an integration domain ranging from the surface of the star, labelled by r=1 in the non-dimensional units and where we imposed boundary conditions, to a distance of five stellar radii, corresponding to r=5. Although this distance is much less than the usual supposed extension of an accretion disk ($\sim$ 100 or 1000 stellar radii) it is far enough to ensure that the solution follows there the asymptotic laws given by Shakura & Sunyaev (1973).

Since some of the physical quantities are to vary steeply in the region very close to the star, we took an exponentially distributed grid of 500 points from r=1 to r=5. Such a dense grid was necessary in order to have a good accuracy in the energy balance in some cases, but was sometimes an oversampling. Anyway, the calculations run quickly provided that we take as an initial state a configuration which is not too different from the one we need. So we proceeded by iterations from a test case, varying parameters.

In the course of the calculations, we had to decide where the boundary layer is, in order to apply a different viscosity prescription there. We chose to change the viscosity prescription according to the gradient of the rotation rate. In other words, the viscosity presents a discontinuity when the couple is zero. Hopefully, this should not disturb too much neither the calculation nor the physics since ν always appears as $\nu\partial_R\Omega$, thus smoothing the effect of the discontinuity. A continuous formula for the viscosity which bridges the two regimes could also have been applied (see Papaloizou & Stanley 1986) but this would have complicated the linearization without changing the results very much.

3. Results

3.1. General features

The asymptotic behaviour of all the variables follows very strictly the standard analytic laws, until they are perturbed by the boundary layer effect. We verify also that the assumptions we made to solve the equations are not violated: the structure is everywhere optically thick and geometrically thin, including in the boundary layer. The typical ratio H/R given by $\mathscr{M}_{dim}^{-1}$ is very close to the real value, a few percents in every cases. There are two prominent features in the results we obtain.

First is the presence of a twofold boundary layer. This was already noticed by Narayan & Popham (1993). The first one, of width $\delta_{visc} = \dfrac{R_{visc}}{R_\star} - 1$, is determined by the maximum of the rotation rate. This is the usual definition and we shall refer to it as the viscous boundary layer. But it appears very clearly that the temperature behaves differently. It also shows a boundary layer profile near the star, but with a totally different length scale $\delta_{th} = \dfrac{R_{th}}{R_\star} - 1$. This is the thermal boundary layer. According to the standard model, the temperature has to drop near the center for values of $\mathscr{C}$ close to 1. But the presence of the boundary layer makes it rise again. Thus there is a point where the temperature presents a minimum, just after deviating from the standard profile. That is where we *defined* the thermal boundary layer to begin. This definition is in accordance with the one for the viscous boundary layer, bounded by the location of zero derivative for the rotation rate. This effect is in fact not surprising and happens whenever conduction is combined with viscosity. In usual hydrodynamics, where conductivity and viscosity are constant and the fluid incompressible, one can easily define the constant Prandtl number:

$$\mathscr{P} = \frac{C_p \nu \varrho}{\chi},$$

where C_p is the thermal capacity at constant pressure, ν, the constant viscosity and χ, the constant thermal conductivity. This number characterizes the relative importance of viscous diffusion with respect to conductive diffusion, and allows to describe the general features of the viscous boundary layer and the thermal boundary layer. For high Prandtl numbers, viscous diffusion is faster; hence forth, the transport of momentum is more efficient and the velocity profile near the boundary has a larger length scale than the temperature profile. Exactly the reverse occurs for small Prandtl numbers. An order-of-magnitude estimation can be made for the ratio of these two thicknesses (Guyon et al. 1991):

$$\frac{\delta_{visc}}{\delta_{th}} = \mathscr{P}^{1/3}$$

in the case of high Prandtl numbers, and

$$\frac{\delta_{visc}}{\delta_{th}} = \mathscr{P}^{1/2} \tag{11}$$

in the case of low Prandtl numbers.

Here we deal with a much more complex fluid, but we can nevertheless make an analogy. In fact, a gas coupled with radiation in the diffusion approximation has an effective conductivity

$$\chi = \frac{16\sigma}{3}\frac{T^3}{\kappa\varrho}.$$

So we face a fluid that is compressible and whose viscosity and diffusion coefficient strongly depend on temperature and density. This strong feedback makes any prediction very hazardous. However, the effective Prandtl number defined above computed with the relevant quantities for a standard accretion disk happens to be a constant: if one takes the Shakura & Sunyaev (1973) profiles, the physical quantities follow the relations:

$$\Sigma\nu = \frac{\dot{M}}{3\pi}(1 - \mathscr{C}\sqrt{\frac{R_\star}{R}})$$

$$\sigma {T_{eff}}^4 = \frac{32\sigma T^4}{3\tau} = \frac{3GM\dot{M}}{8\pi R^3}(1 - \mathscr{C}\sqrt{\frac{R_\star}{R}})$$

with the definition: $\tau = \kappa\Sigma$. Besides,

$$C_p = \frac{\gamma}{\gamma - 1}\frac{k_B}{\mu} = \frac{\gamma}{\gamma - 1}\frac{C_s^2}{T},$$

where k_B is the Boltzmann constant and C_s the isothermal sound speed.

Thus, the Prandtl number reads, using

$$\varrho = \frac{\Sigma}{2H} \text{ and } H = \frac{C_s}{\Omega_K}$$

$$\mathscr{P} = \frac{\gamma}{\gamma - 1}\frac{4}{9} = \frac{10}{9},$$

if $\gamma = \frac{5}{3}$.

Of course, this is no more true in the boundary layer where a different viscosity prescription is applied and where we don't know the temperature and density profiles *a priori*. What is in fact expected is that the Prandtl number will be smaller in the boundary layer, due to the smaller viscosity. The relevant Prandtl number is estimated using the boundary layer viscosity and is thus:

$$\mathscr{P}_{BL} = \frac{C_P \nu_{BL} \varrho}{\chi} \sim \frac{\mathscr{P}}{\mathscr{M}_{dim}} \text{ or } \frac{\mathscr{P}}{\mathscr{M}_{dim}^2},$$

depending on which prescription we apply. Hence the Prandtl number will only loosely estimate the ratio of the two thicknesses, but its magnitude will indicate at least which one is larger. Typical numerical values lead one to suspect that the thermal boundary layer will be much larger than the viscous one, what actually occurs. Figure 1 is a plot of effective Prandtl numbers in our simulations. In this example, the parameters are those of a T-Tauri star and we varied the constant $\mathscr{C}$ from 0.99 to 1.01. The discontinuity is due to the change of viscosity prescription, as explained above (Sect. 2.3). The ratio $\delta_{visc}/\delta_{th}$ ranges from 23.3 ($\mathscr{C}$ = 1.01) to 15.3 ($\mathscr{C}$ = 1) and 9.7 ($\mathscr{C}$ = 0.99), satisfying eq. 11 in order of magnitude. The effective Prandtl number is much lower than one even in the thermal boundary layer, where the "standard" boundary layer viscosity prescription is applied.

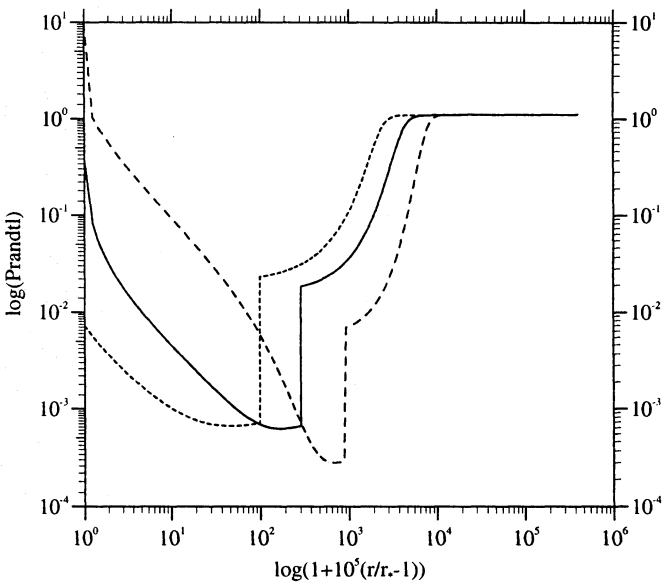

Fig. 1. Plot of the effective Prandtl number with T-Tauri parameters with three different values of $\mathscr{C}$: 0.99 (long dashed line), 1 (solid line) and 1.01 (short dashed line). The discontinuity corresponds to the change in viscosity prescription and thus to the location of the viscous boundary layer

A second important feature is the presence of a radial energy flux at the inner boundary. Again, this has been noticed already by Regev (1983). The new fact is that this flux can be on either sign, depending on physical parameters in the disk. The basic physical process is as follows: the boundary layer temperature tends to settle at a "natural" value, fairly independent of the boundary temperature and governed only by the boundary layer geometry. At the boundary, the disk meets the star and, if the temperatures do not match, a radial flux is generated, due to a strong temperature gradient. Thus, if the boundary (star) temperature is low, the radial flux is negative and directed *into* the star. On the contrary, if the star is hot, the radial flux is positive and the star feeds the boundary layer with radiative energy. There is of course an intermediate case where the radial flux is zero and no radiative energy transfer occurs between the star and its accretion disk. The presence of this radial flux has a great influence on the energy budget of the whole system.

3.2. Energetics

The standard theory assumes that the disk and the boundary layer equally share the total gravitational energy: $L_{acc} = \frac{GM\dot{M}}{R_\star}$. It has been noticed for some time and by several authors that it is no more the case when a true boundary layer is present, even very thin, and also if the rotation rate of the central object is not zero. Recent papers, for instance Kley (1991), Duschl & Tscharnuter (1991), Glatzel (1992), tackle the problem of accurately treating the energy dissipation in the disk and the boundary layer. However, we would like to emphasize that dissipated energy and luminosity should not be mixed up. In the disk itself, where the radial energy flux can be neglected, the approximation of immediate radiation of locally dissipated energy is correct. But in the boundary layer, where the radial transport of radiative energy becomes important, this approximation breaks down. What is effectively radiated out locally, that we call luminosity because it is the real observable energy, is the vertical flux, whereas the radial flux merely transports radiative energy from one location to the next, without giving place to any radiation that one can observe in the first place. This point has already been raised by Regev (1983) and Bertout & Regev (1992).

We present in Appendix an analytic calculation, analogous to the one derived by Kley (1991), but taking into account all the terms, including the advection of energy and the radial flux. The result is the following in non-dimensional form:

$$\begin{aligned}\frac{L_{bl}}{L_{acc}} &= \frac{\int_{R_\star}^{R_{th}} 2\pi R 2F_z(R)\, dR}{L_{acc}} \\ &= [-\frac{1}{r} - \frac{r^2\omega^2}{2} + \mathscr{C}\omega - \frac{2}{\mathscr{P}_{dim}\mathscr{M}^2_{dim}} rhf_r \\ &- \frac{1}{\mathscr{M}_{dim}}(ru_r p) + \frac{1}{\mathscr{M}^2_{dim}}(\frac{u_R^2}{2} + t)]_1^{r_{th}} \end{aligned} \quad (12)$$

An identical formula is of course valid for the disk, but the integration boundaries are r_{th} and r_{disk}. The last three terms in Eq. 12 are negligeable and can be dropped to give a simpler expression. In this approximation, the first three terms of equation represent the contribution of the dissipation, the term including f_r, the one of the radial flux. The latter happens to be important in the boundary layer and has been forgotten in previous calculations.

The following formulae thus stand for the energy balance in the boundary layer and in the disk:

$$L_{BL} = L_{diss}(BL) + L_r(R_\star) - L_r(R_{th}) \quad (13)$$

$$L_{disk} = L_{diss}(disk) + L_r(R_{th}) - L_r(R_{disk})$$

With our definitions, $L_r(R_{th})$ is zero and $L_r(R_{disk})$ can be neglected, leading to the usual approximation for the disk (dissipation=radiation) and a different one for the boundary layer:

$$L_{BL} = L_{diss}(BL) + L_r(R_\star).$$

As a consequence, the boundary layer radiates exactly what is dissipated in it only when there is no radial flux. The normalized dissipated energy can also be calculated by the usual integral:

$$\begin{aligned}\frac{L_{diss}}{L_{acc}} &= \frac{2\int_{R_\star}^{R_{th}} 2\pi R \left(0.5\nu\Sigma (R\partial_R\Omega)^2\right)\, dR}{L_{acc}} \\ &= \int_1^{r_{th}} \nu\Sigma r^2 \partial_r\omega^2 dr. \end{aligned} \quad (14)$$

It is easy to verify that the dissipated energy can be written, to first order in δ_{th} and assuming that $\omega_{th} = r_{th}^{-3/2}$, (or $\delta_{th} > \delta_{visc}$), as:

$$\frac{L_{diss}}{L_{acc}} = \frac{(1-\omega_\star)^2}{2} + (1-\mathscr{C})(\omega_\star - 1 + \frac{3\delta_{th}}{2}). \quad (15)$$

This last formula is identical to the one derived by Kley (1991), except that the boundary layer thickness δ_{th} refers to the thermal boundary layer, and that it gives the *dissipated* energy and not the luminosity.

This is a point of discussion whether the radial luminosity could be observable directly and thus take part to the boundary layer luminosity. In particular, when the star is heated by the boundary layer, Bertout & Regev (1992) propose that this energy may heat a circle around the star that can eventually radiate away and may then be accessible to observation. But there are obviously several scenarii that one may think of for the final release of this radial energy. It may simply heat the outer layers of the star without penetrating deeply inside and be reradiated on the spot, or participate in some way to the global energy balance of the star. It may also create an local overpressure and initiate a wind or even a jet. This point will remain speculative in absence of a real dynamical as well as thermal coupling of the star and its surrounding boundary layer. The model presented in this paper cannot deal with the detailed interaction of the star and and the surrounding material. We shall assume that the radial luminosity is included in some way in the stellar appearance and does not influence the boundary layer luminosity, defined to be the energy radiated vertically.

We should stress here that the local energy budget of the gas is the balance between two terms. In the disk, of course, the dissipation is compensated by the vertical radial flux. In the intermediate region bounded by the maximum of the rotation rate and the thermal boundary layer the radial and vertical fluxes are dominant, while in the innermost regions, the dissipated energy is transported by the radial flux. Thus, the advection and compression terms seem to be negligible everywhere.

3.3. Radial profiles in the boundary layer

All the radial profiles have the same qualitative aspect: a twofold boundary layer, with a ratio of the two thicknesses ranging from 10 to 100. The thermal boundary layer extends typically on a few percents of the stellar radius while the viscous boundary layer has a width of a few thousandths of the stellar radius. When

the viscosity prescription in the boundary layer is of the type given by Shakura & Sunyaev (1988) or Regev (1983), we have $\delta_{visc} \sim$ a few $10^{-4} R_\star$. All the curves are perfectly continuous, although the viscosity is not.

The parameters involved can be separated into two groups: the mere boundary conditions, like $\Omega_\star$ or $T_\star$, and those more intrinsic to the physics of the disk: $\dot{M}$, α, $\mathscr{C}$.

For the latter group of parameters, their influence on the profile of physical quantities in the disk is well-known, given an opacity law. In the boundary layer, the dependence remains qualitatively identical, although magnified, because the rate of energy dissipation is much higher.

The most spectacular variations occur with the constant $\mathscr{C}$ (see Fig. 2). Mild in the disk, because it is not supposed to depart very much from 1, the influence of $\mathscr{C}$ is dramatic on the boundary layer. A one percent variation induces a variation of almost an order of magnitude for the boundary layer thickness, and consequently a large factor on the temperature. This result may be interpreted geometrically as follows: $\mathscr{C}$ is in fact a boundary condition for the angular momentum diffusion equation. Thus, it links the value the rotation rate at the boundary with its derivative. Hence, one clearly understands its influence on the geometry of the boundary layer. Looking at the equation 7, it is clear that the smaller $\mathscr{C}$, the smaller $\partial_R \Omega$. Thus, the boundary layer will be larger for a smaller $\mathscr{C}$, and consequently will radiate more. As the boundary layer cannot radiate more than what is dissipated in it (when no extra energy source is present), there is a lower limit for $\mathscr{C}$. Since the boundary layer geometry is very sensitive to the value of $\mathscr{C}$, this limit is close to 1 (see Fig. 9).

The effect of the accretion rate $\dot{M}$ is displayed on Fig. 3. $\dot{M}$ is the only parameter in this comparative study which influences the accretion luminosity and the constant $\mathscr{M}_{dim}$. Although we varied $\dot{M}$ by an order of magnitude around a "standard" value, its influence on the boundary layer thickness is much lower than $\mathscr{C}$. We clearly see the effect of the boundary temperature on the temperature profile on the boundary layer in the case of low $\dot{M}$ (dotted line). In that case, the boundary layer radiates more than if the accretion rate were higher, because the radial flux is positive.

The α parameter does not have any influence on the disk appearance. However, it alters the central temperature and hence the radial flux at the boundary and the boundary layer luminosity. As α rises, the temperature profile in the boundary layer flattens, and becomes eventually a decreasing function of the radius (see Fig. 4). Notice by the way that the viscous boundary layer thickness, corresponding to a higher value of $\mathscr{M}_{dim}$ given by the white dwarf set or parameters, is roughly one order of magnitude lower than the one calculated by with the T-Tauri set. The thermal boundary layer is only two or three times thinner. Notice also, that the boundary layer is about to be optically thin for higher values of α. We are at the limit of our approximations.

In every of the three former cases, the natural variation of the central temperature with a given parameter is constrained by the boundary temperature, which thus acts as a lower limit on the boundary layer temperature.

Table 2. Comparison of δ_{visc} and the typical local size of the turbulent eddies: $\frac{H^2}{R^2}$ for the curves of Fig. 6.

viscosity prescription	δ_{visc}	$\frac{H^2}{R^2}$
$\nu_{BL} = \alpha C_s H^2/R$	$2.83\ 10^{-3}$	$1.26\ 10^{-3}$
$\nu_{BL} = \alpha C_s H^3/R^2$	$7.86\ 10^{-5}$	$8.29\ 10^{-4}$
$\nu_{BL} = \overline{\nu_{disk}}/\mathscr{M}^2_{dim}$	$2.72\ 10^{-4}$	$9.24\ 10^{-4}$

The star rotation rate has a small influence on the profiles but of course the total dissipated energy in the boundary layer depends on it and also the spectral distribution of the emitted energy. It is not surprising that smaller rotation rates lead to higher temperatures in the boundary layer (Fig. 5).

The size of the viscous boundary layer is obviously linked to the viscosity contrast between the disk and the boundary layer. This was noticed by Glatzel (1992): the greater the viscosity contrast, the thinner the boundary layer. Figure 6 displays profiles with the three different viscosity prescriptions described in Sect. 2.3. The thinnest boundary layer results from the constant viscosity, more than one order of magnitude thinner than for the "standard" boundary layer viscosity prescription. The same qualitative behaviour with the model parameters occurs with the Shakura & Sunyaev (1988) prescription (or also the Regev (1983) prescription), but the boundary layer remains much colder, and hence radiates much less. The consistancy of the model can be checked also by comparing δ_{visc} and $\frac{H^2}{R^2}$. For the curves of Fig. 6, we give the numbers in Table 2. This shows that the "standard" boundary layer viscosity prescription leads to consistent results, because the typical size for the turbulent eddies is of the order of the viscous boundary layer thickness, or smaller. On the contrary, for the two other prescriptions, the typical length scale for the eddies in the boundary layer is larger than δ_{visc}, up to an order of magnitude. This is an objection to these two prescriptions.

3.4. Luminosities

Thanks to our self-consistent calculations, we have been able put numbers in the analytical formula (eq. 12) and compare it to the integral calculated numerically (eq. 14). We found an agreement of a few tenths of a percent, which is a good check for the numerical results. We present in Fig. 7 and Fig. 8 the dependence of the vertical emission of the boundary layer and the radial luminosity with α at fixed boundary temperature and with $T_\star$ at fixed α. These plots clearly show that most of the accretion luminosity is radiated into the star when the boundary temperature is low, the boundary layer luminosity being only of the order of a few percents of the accretion luminosity. Rising the temperature increases the boundary layer luminosity at the expense of the radial flux. Eventually, the latter becomes positive, and the accretion luminosity is no more relevant for the global energy balance, since the star is a source of energy for

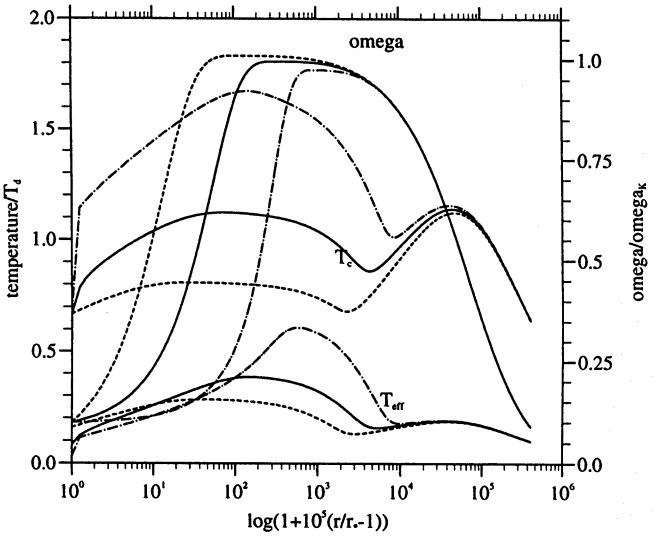

Fig. 2. Plot of the scaled temperature, effective temperature and rotation rate, with the T-Tauri parameters with three different values of $\mathscr{C}$: 0.99 (dot dashed line), 1 (solid line) and 1.01 (dashed line). T_{dim}=7510K

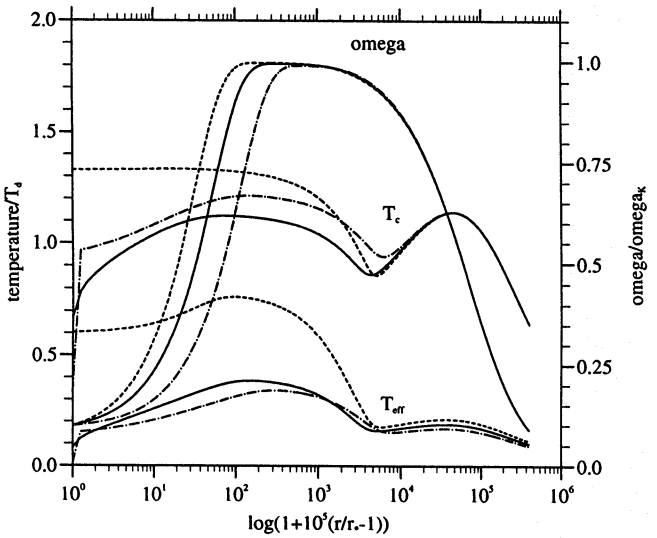

Fig. 3. Plot of the scaled temperature, effective temperature and rotation rate, with the T-Tauri parameters and three different values of $\dot{M}$: $10^{-8}M_{\odot}yr^{-1}$ (dashed line), $10^{-7}M_{\odot}yr^{-1}$ (solid line) and $10^{-6}M_{\odot}yr^{-1}$ (dot-dashed line). The scaling makes the curves identical in the disk, and displays the *relative* influence of $\dot{M}$ in the boundary layer. T_{dim}=3760K, 7510K and 15000K, respectively

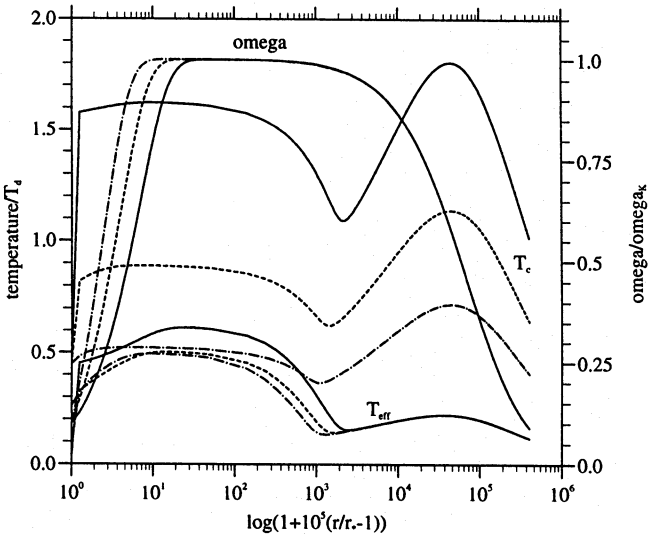

Fig. 4. Plot of the scaled temperature, effective temperature and rotation rate, with the white dwarf parameters and three different values of α: 10^{-3} (solid line), 10^{-2} (dashed line) and 10^{-1} (dot-dashed line). T_{dim} = 2.23 10^5K

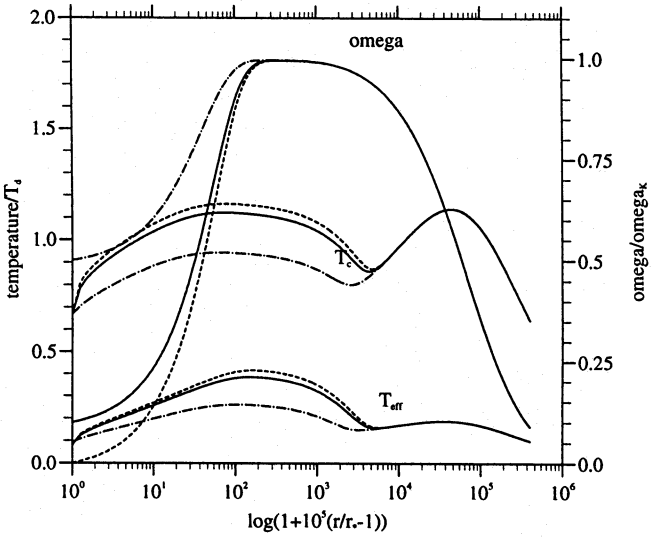

Fig. 5. Plot of the scaled temperature, effective temperature and rotation rate, with the T-Tauri parameters and three different values of $\omega_{\star}$: 0 (dashed line), 0.1 (solid line) and 0.5 (dot-dashed line). T_{dim}=7510K

the disk. The great sensitivity of the boundary layer luminosity to the boundary temperature is also to be noted and suggests that the outer layers of the star should either be stabilized at a given temperature or oscillate around it.

One can draw some general laws, which can be qualitatively understood and that enlighten the global behaviour of such complex objects. For high boundary layer central temperatures, the effective temperature is also high (for an opacity law decreasing with temperature) and so is the luminosity. The luminosity then decreases with temperature until it reaches the vicinity of the boundary temperature, where the luminosity rises again because extra energy comes from the star. This is illustrated in Fig. 9, where we see this typical dependence of the boundary layer luminosity with the constant $\mathscr{C}$. The same discussion holds for every parameter "intrinsic" to the disk physics (α, $\dot{M}$), but is not always so clear.

Table 3. Values of the boundary layer luminosity and width for different cases, displayed in Fig. 10 .

Fig 10	v	ariable parameter	L_{BL}/L_{acc}	$\delta_{th}(\%)$	Comments
		0.98	$1.37\ 10^{-3}$	2.37	
		1.00	$1.44\ 10^{-4}$	0.62	TTauri
10a	$\mathscr{C}$	1.02	$4.66\ 10^{-3}$	2.23	$\nu_{BL} = \alpha C_s H^3/R^2$
		1.025	$2.55\ 10^{-2}$	2.86	
		10^{-3}	$6.51\ 10^{-3}$	1.76	WD
10b	α	0.01	$1.16\ 10^{-2}$	1.58	$\nu_{BL} = \alpha C_s H^2/R$
		0.05	0.190	2.22	$T_\star = 2\ 10^5$K
		$\alpha C_s H^2/R$	$1.16\ 10^{-2}$	4.33	
10c	ν_{BL}	$\alpha C_s H^3/R^2$	$1.44\ 10^{-4}$	0.62	TTauri
		$\overline{\nu_{disk}}/\mathscr{M}^2_{dim}$	$6.46\ 10^{-4}$	1.35	$\alpha = 10^{-2}$
		$10^{-6} M_\odot yr^{-1}$	$2.80\ 10^{-2}$	6.19	TTauri
10d	$\dot{M}$	$10^{-7} M_\odot yr^{-1}$	$1.84\ 10^{-2}$	4.33	$\nu_{BL} = \alpha C_s H^2/R$
		$10^{-8} M_\odot yr^{-1}$	0.135	5.06	$\alpha = 10^{-2}$
		2500K	$1.53\ 10^{-3}$	3.44	TTauri
10e	$T_\star$	5000K	$2.64\ 10^{-2}$	3.94	$\nu_{BL} = \alpha C_s H^2/R$
		7500K	0.652	7.25	$\alpha = 10^{-1}$
		0.0^3	$2.59\ 10^{-3}$	4.72	TTauri
10f	$\omega_\star$	0.2	$1.28\ 10^{-2}$	3.94	$\nu_{BL} = \alpha C_s H^2/R$
		0.5	$3.30\ 10^{-3}$	2.62	$\alpha = 10^{-2}$

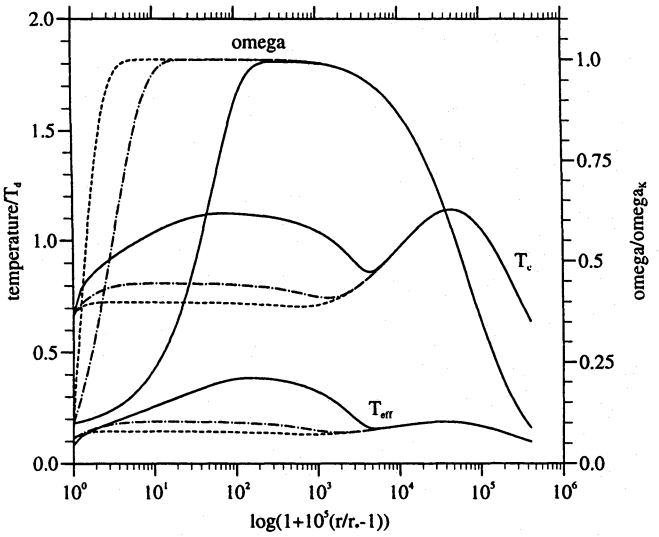

Fig. 6. Plot of the scaled temperature, effective temperature and rotation rate, with the T-Tauri parameters and three different viscosity prescriptions: $\nu_{BL}= \alpha C_s H^2/R$, (solid line), $\overline{\nu_{disk}}/\mathscr{M}^2_{dim}$ (dashed line) and $\alpha C_s H^3/R^2$ (dot-dashed line). T_{dim}=7510K

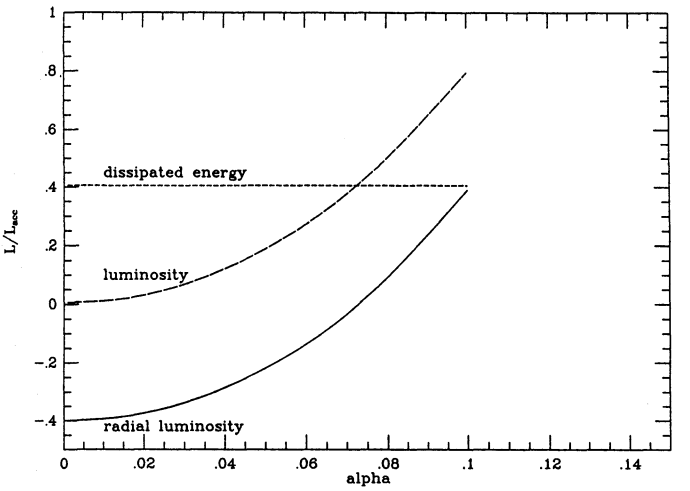

Fig. 7. Plot of the boundary layer luminosity, radial luminosity and dissipated energy in the boundary layer, with the T-Tauri parameters, against α

4. Observational implications

4.1. Spectral distribution

We can have an idea of the emitted spectrum of an accreting object by studying the spectral distribution of its total luminosity. Of course, the effects of geometry like inclination angle, shadowing, reprocessing can only be computed in special cases. We worked out one example of this kind in the following section. The spectral distribution of the structure we calculated are given by the following classical formula, assuming that the emission is everywhere that of a blackbody at the local effective temperature, which we write in non-dimensional form:

$$\frac{2\int_{R_\star}^{R_{th}} 2\pi R dR \pi \lambda F_\lambda}{L_{acc}} = \frac{45}{2\pi^4 \overline{\lambda}^4} \int_1^{\tau_{th}} \frac{r dr}{e^{\overline{\tau}^{1/4}/\overline{\lambda}t} - 1}$$

where $\overline{\lambda}$ is a scaled wavelength:

$$\overline{\lambda} = \frac{\lambda}{\lambda_{dim}}$$

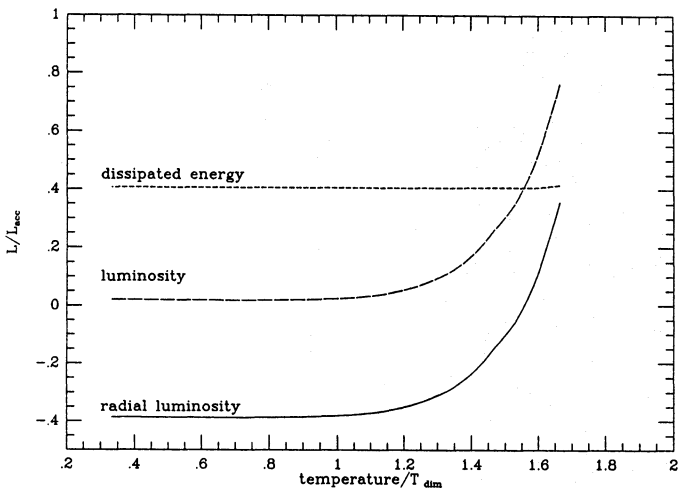

Fig. 8. Plot of the boundary layer luminosity, radial luminosity and dissipated energy in the boundary layer, with the T-Tauri parameters, against $T_\star$

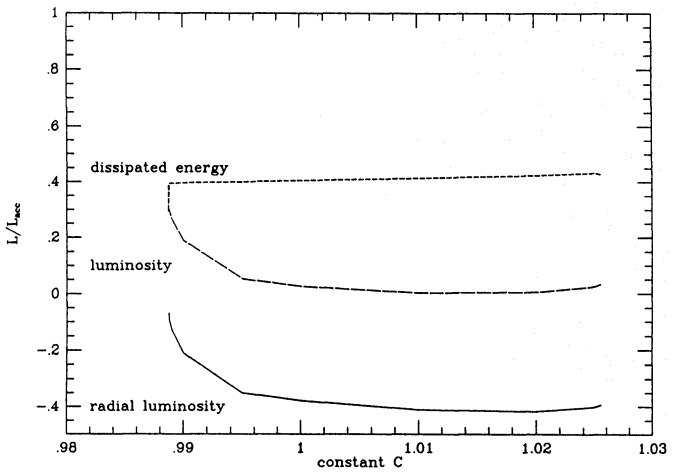

Fig. 9. Plot of the boundary layer luminosity, radial luminosity and dissipated energy in the boundary layer, with the T-Tauri parameters, against constant $\mathscr{C}$

with

$$\lambda_{dim} = \frac{ch}{k_B}\left(\frac{8\pi\sigma R_{dim}^3}{3GM\dot{M}}\right)^{1/4},$$

and $\overline{\tau}$, the scaled optical depth.

Thus, scaling the outgoing flux by L_{acc} and the wavelengths by λ_{dim} allows us to present the results in a unified way. The disk spectrum is a universal function whereas the boundary layer spectral distribution is a deviation from this. We can thus directly compare the relative influence of different parameters and the respective high energy excess for different astrophysical objects. We plotted in Fig. 10 the spectral distribution obtained for various different cases. Let us recall again that these spectral distributions are obtained by analysing *only* the vertical radiative flux. Looking at the plots, it seems that different configurations can lead to similar observational appearance, unless parameters can be otherwise constrained. This rises the question of the uniqueness of a given interpretation of observed spectra addressed by Basri & Bertout(1989). It is to be noted that the more realistic cases correspond to fairly *low* boundary layer luminosities, of the order of a few percents of the accretion luminosity.

4.2. A worked example

As an example, we calculated with the method described in this paper the radial profiles and the outgoing spectrum of the system DF Tau studied in detail by Bertout et al. (1993). They calculated from their best fit model the ranges of different parameters for the system. In our case, δ, the boundary layer thickness, is calculated self-consistently, so that we don't have to fix it. We took into account the rotational constraints linking $R_\star$ and the inclination angle, i. We took $\dot{M}$ according to the range they give. These parameters fix the shape of the spectrum at long wavelengths and the scaling of the photospheric contribution. We suppose that the boundary temperature is the effective temperature of the star ($\sim$ 2500 K) and we took $\nu_{BL} = \alpha C_s H^2/R$. After that, we still have two free parameters, the viscosity coefficient, α, and the constant $\mathscr{C}$. We took the more realistic grey opacity law given by Lin & Papaloizou (1985). The set of parameters displayed in Table 4 gave a reasonable fit to the data.

We did not use a χ^2 method, so we are not sure to achieve a "best fit" in the usual sense, but the feasibility of such a simulation is shown. In particular, the calculation of the spectrum of the boundary layer should include self-consistently estimated opacities and optical depths. In principle, it could be possible to reproduce the Balmer jump for instance with a better radiative transfer. A better fit of the high wavelength part could be obtained by varying the disk extent, what is technically straightforward, and we postpone this improvement to a forthcoming study together with a wavelength dependent radiative transfer in the boundary layer. We end up with a best value for α of 0.15, fairly lower than the one found in Bertout et al. (1993), a larger boundary layer (δ = 0.073) and a very low luminosity:

$$\frac{L_{BL}}{L_{acc}} = 0.115,$$

the rest being radiated into the star:

$$\frac{|L_R(R_\star)|}{L_{acc}} = 0.286.$$

Note that the boundary layer luminosity quoted above is the total luminosity, uncorrected for geometrical effects (shadowing by the star). The apparent luminosity reaching the observer, given by the integral of the curve on Fig. 11, is:

$$\frac{L_{BL_{app}}}{L_{acc}} = 0.032.$$

Note that the apparent luminosity of the boundary layer is roughly one fourth of its total luminosity, which is to be expected. The statement we made in the preceding section is

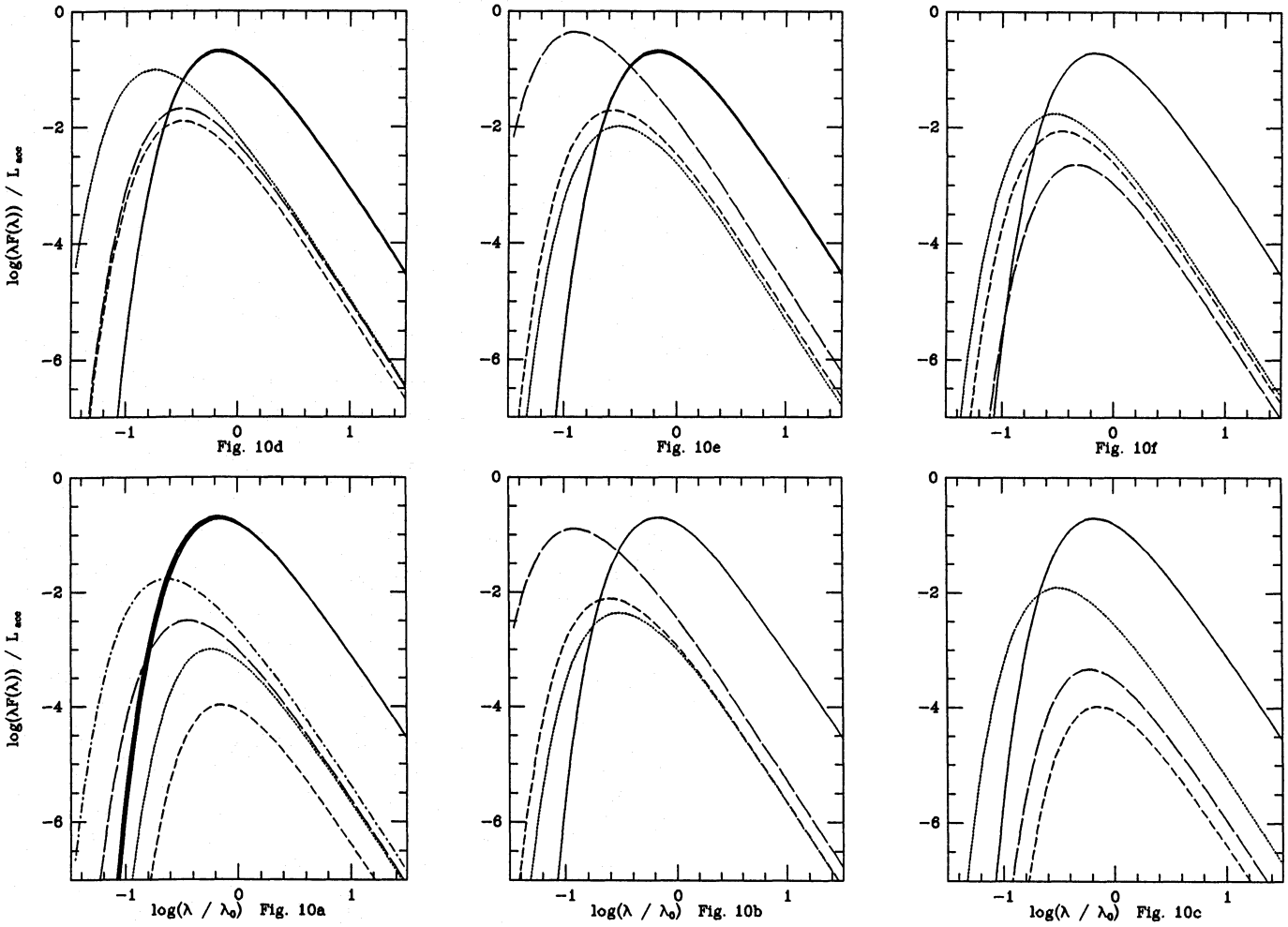

Fig. 10. Plot of the normalized spectral distribution of the disk and boundary layer in different cases. Numerical details are listed in Table 3. The solid line corresponds to the disk contribution. There is a slight dispersion in the disk spectra because it does not have exactly the same extent in each case. The other lines display the boundary layer contribution. Fig. 10a: $\mathscr{C}$= 0.98 (dotted line), $\mathscr{C}$= 1 (short dashed line), $\mathscr{C}$= 1.02 (long dashed line), $\mathscr{C}$= 1.025 (dot-dashed line). Fig. 10b: $\alpha = 10^{-3}$ (dotted line), $\alpha = 10^{-2}$ (short dashed line), $\alpha = 5\ 10^{-2}$ (long dashed line). Fig. 10c: $\nu_{BL} = \alpha C_s H^2/R$ (dotted line), $\nu_{BL} = \alpha C_s H^3/R^2$ (short dashed line), $\nu_{BL} = \overline{\nu_{disk}}/\mathscr{M}^2_{dim}$ (long dashed line). Fig. 10d: $\dot{M} = 10^{-8} M_\odot yr^{-1}$ (dotted line), $\dot{M} = 10^{-7} M_\odot yr^{-1}$ (short dashed line), $\dot{M} = 10^{-6} M_\odot yr^{-1}$ (long dashed line). Fig. 10e: $T_\star$ = 2500 K (dotted line), $T_\star$ = 5000 K (short dashed line), $T_\star$ = 7500 K (long dashed line). Fig. 10f: $\omega_\star = 0$ (dotted line), $\omega_\star = 0.2$ (short dashed line), $\omega_\star = 0.5$ (long dashed line)

here exemplified: a small fraction of the accretion luminosity is enough to explain the UV excess of the spectrum of DF-Tau. Hence, the boundary layer intrinsic luminosity is low compared to the dissipated energy. As a result, radiative energy is free to stream into the star and be reprocessed in some way.

5. Discussion and conclusion

Although very simple and following directly the standard one, our model shows striking features that had not been noticed clearly so far (the presence of radiative diffusion in the boundary layer leads to a strong radial flux at the boundary and an extended thermal boundary layer with respect to the viscous boundary layer), and a physical discussion on the influence of various model parameters. A complete example has been worked out, taking into account more physics like the geometry of the object, reprocessing and shadowing.

As we mentioned in the introduction, our model differs from the one by Narayan & Popham (1993) mainly by the boundary conditions and the assumption of optical thickness everywhere. When optically thick, their solutions are always hotter than ours, meaning that the central temperature is always higher than the one in the inner layers of the disk, with a runaway at the boundary. On the contrary, in our solutions the central temperature of the boundary layer is almost always *lower* than in the disk, leading to *cool* boundary layers, already discussed in Bertout & Regev (1992). As a consequence, the matching of the radiative flux of a star is correct in their case, but the temperature might not be satisfactory. This problem is to be added to the geometrical one we quoted in the introduction.

Table 4. Values of the model parameters for DF-Tauri.

i	α	$T_\star$	$\dot{M}$	$\mathscr{C}$	δ_{th}	L_{BL}/L_{acc}
60	0.15	2500 K	1.2 $10^{-7} M_\odot/yr$	0.992	7.3%$R_\star$	0.115

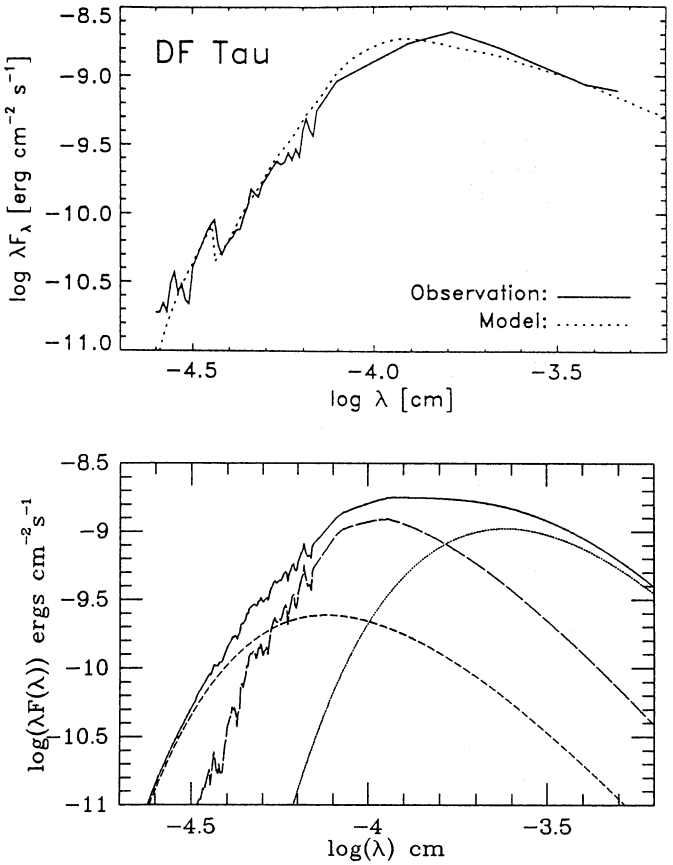

Fig. 11. Here is the observed spectral distribution of star DF-Tauri (top, from Bertout *et al.* (1993)) along with our own simulation of the same object (bottom). The three components of the global spectrum are also displayed (disk, boundary layer and star)

Of course, many physical processes are crudely treated and should obviously be improved. A more realistic opacity law and a more refined radiative transfer, especially in the vertical direction, would be highly desirable to produce a better spectrum of the boundary layer. The effect of chemistry and the variation of the mean molecular weight should be included. Much more difficult would be to take into account magnetic fields, a probably very important ingredient of the accretion phenomenon. This is still an unclear technical point to understand how the choice of boundary conditions (central temperature versus central flux for example) influences the final results, and which one is more realistic. A better understanding of the disk-star interaction could be of some help to answer that question. Unfortunately, this interaction is simulated very crudely in this kind of stationary calculations. First of all, assuming a constant accretion rate is always conflicting with an hydrostatic young star since the velocities of the disk don't cancel at the boundary. Second, the very strong effect of the boundary temperature on the energetics of the boundary layer is worrying for the existence of a stationary state at all.

It might be very difficult to disentangle the influence on the outgoing spectrum of different parameters since they can give so similar spectral distributions; in particular, we found very difficult to exclude one viscosity prescription in favour of the other, except for the fact that the mean luminosity is higher for a higher viscosity in the boundary layer, and that the viscosity prescription proposed by Shakura & Sunyaev (1988) or Regev (1983) might be inconsistent. The very strong influence of the total accreted angular momentum is a quite a new fact and a precise study of the history of the rotation rate of young stars or white dwarfs may provide useful information. Once again, a theoretical study of the angular momentum tranfer to the star would need a better knowledge of the star-disk interaction, and possibly require non-stationary simulations. Another striking result is that the observed boundary layer luminosities are quite low, and are thus compatible with an ingoing radiative flux. This may be in favour of the fact that the radial flux does not cancel at the boundary and that the corresponding energy is reprocessed so that it is not directly observable in the high energy part of the outgoing spectrum. Boundary layers and jets could thus coexist.

Acknowledgements. We thank Jérôme Bouvier for providing us with the stellar spectral distribution. The final form of the manuscript owes very much to our referee, Oded Regev, whose relevant comments are warmly acknowledged.

Appendix A: calculation of the boundary layer luminosity

Combining the Eqs. 2 and 3 gives the total energy variation:

$$\frac{-\dot{M}}{2\pi R}\partial_R\left(\frac{u_R^2}{2}+\frac{(R\Omega)^2}{2}-\frac{GM_\star}{R}\right)=$$
$$-u_R\partial_R P+\frac{\Omega}{R}\partial_R\left(\nu\Sigma R^3\partial_R\Omega\right)$$

The right hand side can be rewritten, using the integrated form of the angular momentum transport equation:

$$-\frac{1}{R}\partial_R(PRu_R)+\frac{P}{R}\partial_R(Ru_R)\ -$$
$$\frac{\dot{M}}{2\pi R}\partial_R\left(R^2\Omega^2-\mathrm{C}\Omega\right)-\Sigma\nu R^2\left(\partial_R\Omega\right)^2$$

Thus, gathering the derivatives:

$$\frac{-\dot{M}}{2\pi R}\partial_R\left(\frac{u_R^2}{2}-\frac{(R\Omega)^2}{2}-\frac{GM_\star}{R}+\mathrm{C}\Omega\right)+$$

$$\frac{1}{R}\partial_R\left(Ru_R P\right) = \frac{P}{R}\partial_R(Ru_R) \; - \; \nu\Sigma R^2\left(\partial_R\Omega\right)^2$$

Finally, using the energy equation allows to replace the right hand side of the last equation, and make the radiative fluxes appear:

$$\frac{-\dot{M}}{2\pi R}\partial_R\left(\frac{u_R^2}{2} - \frac{(R\Omega)^2}{2} - \frac{GM_\star}{R} + \mathrm{C}\Omega + U\right)$$
$$+\frac{1}{R}\partial_R\left(2HRF_R + Ru_R P\right) \; = \; -2F_z(R),$$

where U is the internal energy. Integrating over a surface element:

$$\int_{R_1}^{R_2} 2\pi R dR 2F_z(R) =$$

$$\dot{M}\left[\frac{u_R^2}{2} - \frac{(R\Omega)^2}{2} - \frac{GM_\star}{R} + \mathrm{C}\Omega + U\right]_{R1}^{R2}$$
$$-2\pi\left[2HRF_R + Ru_R P\right]_{R1}^{R2}$$

In non-dimensional form:

$$\frac{\mathrm{L_{bl}}}{\mathrm{L_{acc}}} = \frac{\int_{R_\star}^{R_{th}} 2\pi R\, 2F_z(R)\, dR}{\mathrm{L_{acc}}}$$
$$= \left[-\frac{1}{r} - \frac{r^2\omega^2}{2} + \mathscr{C}\omega - \frac{1}{\mathscr{M}_{dim}}(ru_r p)\right.$$
$$\left. + \frac{1}{\mathscr{M}_{dim}^2}\left(-\frac{2rhf_r}{\mathscr{P}_{dim}} + \frac{u_r^2}{2} + t\right)\right]_1^{r_{th}}$$

References

Balbus S.A., Hawley J.F., 1991, ApJ, 376, 214
Basri G., Bertout C., 1989, ApJ, 341, 340
Bertout C., Regev O., 1992, ApJ, 399, L163
Bertout C., Basri G., Bouvier J., 1988, ApJ, 330, 350
Bertout C., Bouvier J., Duschl W.D., Tscharnuter W.M, 1993, A & A, 275, 236
Blumenthal G.R., Yang L.T., Lin D.N.C., 1984, ApJ, 287, 774
Duschl W.J., Tscharnuter W.M., 1991, A & A, 241, 153
Glatzel W., 1992, MNRAS, 257, 572
Guyon E., Hulin J.P., Petit L., 1991, Hydrodynamique Physique, Interéditions/Editions du C.N.R.S.
Horne K., Cook M.C., 1985, MNRAS, 214, 307
Kley W., 1991, A & A, 247, 95
Lin D.N.C., Papaloizou J., 1985, Protostars and Planets, II, p. 981, D.C. Black and M.S. Matthews, eds (Tucson, University of Arizona Press)
Lynden-Bell D., Pringle J. E., 1974, MNRAS, 168, 603
Malbet F., Rigaut F., Bertout C., Léna P., 1993, A & A, 271, L9
Muchotrzeb B., Paczyński B., 1982, Acta Astr, 32, 1
Narayan R., Popham R., 1993, Nature, 362, 820
Okuda T., Mineshige S., 1991, MNRAS, 249, 684
Paczyński, B., 1991, ApJ, 370, 597
Papaloizou J.C., Stanley J.E., 1986, MNRAS, 220, 593
Popham R., Narayan R., 1991, ApJ, 370, 604
Press W.H., Flannery B.P., Teukolsky S.A., Vetterling W.T., 1986, Numerical Recipies, Cambridge University Press
Regev O., 1983, A & A, 126, 146
Sargent A.I., Beckwith S., 1987, ApJ, 323, 294
Shakura N.I., Sunyaev R.A., 1973, A & A, 24, 337
Shakura N.I., Sunyaev R.A., 1988, Adv. Sp. Res., 8, 135

This article was processed by the author using Springer-Verlag LaTeX A&A style file version 3.